NRIAG Journal of Astronomy and Geophysics 6 (2017) 60–67

Contents lists available at ScienceDirect

NRIAG Journal of Astronomy and Geophysics

journal homepage: www.elsevier.com/locate/nrjag

Review article

Liquefaction potential of Nile delta, Egypt

Elsayed Fergany *, Khaled Omar

National Research Institute of Astronomy & Geophysics, Helwan, Cairo, Egypt

ARTICLE INFO

Article history:
Received 11 August 2016
Revised 19 January 2017
Accepted 31 January 2017
Available online 23 February 2017

Keywords:
Microtremor measurements
HVSR
Vulnerability index
Liquefaction
Nile Delta

ABSTRACT

Understanding how sedimentary basins respond to seismic-wave energy generated by earthquake events is a significant concern for seismic-hazard estimation and risk analysis. The main goal of this study is assessing the vulnerability index, K_g, as an indicator for liquefaction potential sites in the Nile delta basin based on the microtremor measurements. Horizontal to Vertical spectral ratio analyses (HVSR) of ambient noise data, which was conducted in 2006 at 120 sites covering the Nile delta from south to north were reprocessed using Geopsy software. HVSR factors of amplification, A, and fundamental frequency, F, were calculated and K_g was estimated for each measurement. The K_g value varies widely from south toward north delta and the potential liquefaction places were estimated. The higher vulnerability indices are associated with sites located in southern part of the Nile delta and close to the branches of Nile River. The HVSR factors were correlated with geologic setting of the Nile delta and show good correlations with the sediment thickness and subsurface stratigraphic boundaries. However, we note that sites located in areas that have greatest percentage of sand also yielded relatively high K_g values with respect to sites in areas where clay is abundant. We concluded that any earthquake with ground acceleration more than 50 gal at hard rock can cause a perceived deformation of sandy sediments and liquefaction can take place in the weak zones of $K_g \geq 20$. The worst potential liquefaction zones ($K_g > 30$) are frequently joined to the Damietta and Rosetta Nile River branches and south Delta where relatively coarser sand exists. The HVSR technique is a very sensitive tool for lithological stratigraphy variations in two dimensions and varying liquefaction susceptibility.

Contents

* Corresponding author.
E-mail addresses: elsayed_fergany@hotmail.com (E. Fergany), khaledyosif2002@yahoo.com (K. Omar).

Peer review under responsibility of National Research Institute of Astronomy and Geophysics.

Production and hosting by Elsevier

http://dx.doi.org/10.1016/j.nrjag.2017.01.004

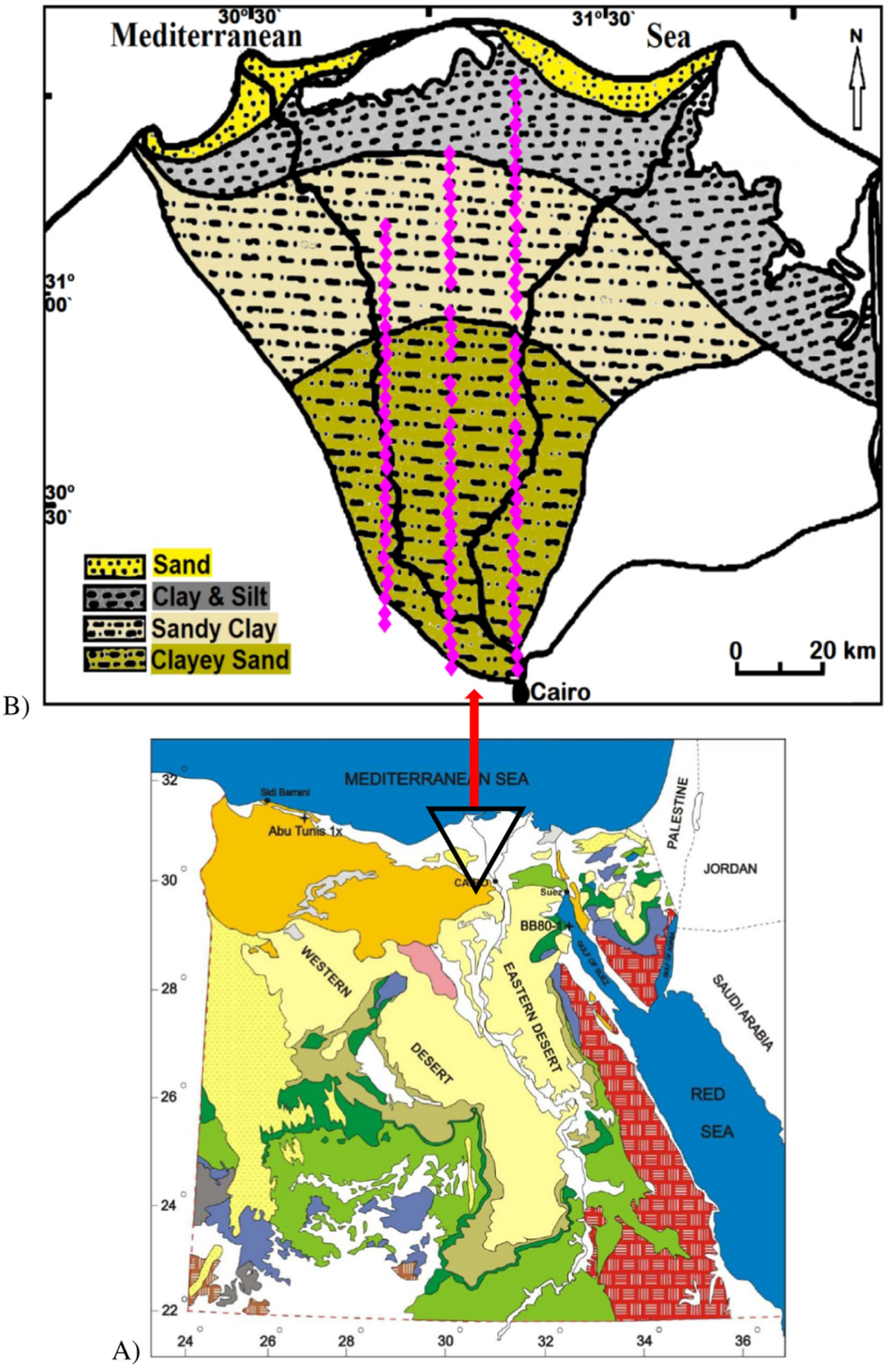

Fig. 1. (A) Egypt map shows study area (black triangle). (B) Study area map shows the distinct lateral variation in the Bilqas formation in the Nile delta (El-Fayoumi, 1987) and three longitudinal lines show microtremor measurements (diamond purple points) used in this study.

1. Introduction

Damages caused by the recent earthquakes are concluded as a direct result of local geological conditions affecting the ground motion (Nakamura, 2000). This effect is controlled by a variety of factors, including proximity to source, rupture characteristics and directivity, acoustic impedance contrasts, near-surface soil properties, and basin structural configuration. Best approach for under-

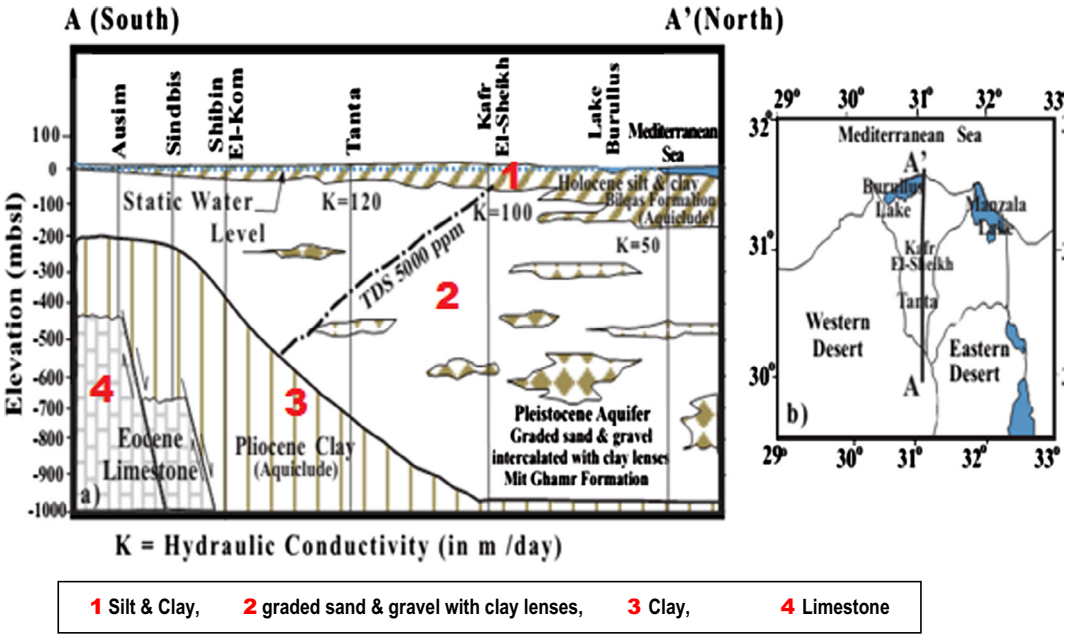

Fig. 2. (a) Longitudinal cross section from south to north of the study area. (b) Key map for cross section (A–A′) (after Elewa, 2010).

standing ground conditions is through direct observation of seismic ground motion, but such studies are restricted to areas with relatively high rates of seismicity. Because of these restrictions in other methods, such as high rates of seismicity and the availability of an adequate reference site, several studies suggest that ambient noise, or weak motions, can be used to identify areas that might amplify earthquake ground motions in advance of earthquake occurrence (e.g., Nakamura, 1989, 1997). After an introduction of the Nakamura's technique (H/V technique; Nakamura, 1989), a renewed great attention was paid for estimating dynamic characteristics of ground and structures using microtremor, since clear and reliable information was provided by very simple and inexpensive noise measurements.

The structure of northern Egypt was built during Oligocene and early Miocene times and has remained since then almost inactive except for minor tremors and earthquakes along some of the older lines (Said, 1981). The potential seismic risk of the Nile delta is due to the amplification of the ground motion caused by the presence of soft basin sediments. The area recently suffered extensive damage and casualties due to a M 5.9 earthquake, occurred on 12 Oct. 1992, located 25 km southwest of Cairo (El-Sayed et al., 1998). The biggest losses were recorded in Cairo and the Nile delta basin. Several thousand people were killed or injured and thousands of buildings were totally collapsed and damaged. Liquefaction was detected in many places at and around the epicentral area. Earthquakes that are located within the Egyptian territory can generate ground acceleration up to 0.15 g (150 gal) in the Nile Delta basin (El-sayed et al., 2001).

In this study, we analyzed the site response using the HVSR method and calculated K_g values based on the microtremor data conducted in 2006 for estimating the potential liquefaction sites in the Nile delta. Data was reprocessed using Geopsy software (2012) to estimate the Amplification (A) and fundamental frequency (F_0) factors for each observation point. K_g index was estimated for each site based on Nakamura (1996, 1997, 2000) technique.

2. Geologic setting

Nile Delta is one of the largest deltas in the world, covering 22,000 km^2 of area (Wright and Coleman, 1973) and represents more than 60% of the inhabited area of Egypt. It begins near Cairo and extends both west and east as it forms the inverted Greek letter delta (Δ) shape that is bounded by the Mediterranean Sea (Fig. 1). The Nile Delta is a wave dominated delta system, as classified by Galloway (1975). It saw three different main avulsions during the Quaternary: the older Proto-Nile, the Pre-Nile, and the Neo-Nile, occurring prior to the modern Nile River flowing today (Rizzini et al., 1978; Said, 1981). The modern Nile Delta reached its current configuration approximately 10,000 years ago (Rizzini et al., 1978). The Delta region can be broadly subdivided into three zones. The first zone is the southern province which constitutes as a portion of the upward zone. This zone is characterized by relatively thin sedimentary cover and by development of the graben - like structure. The second one is the central province which coincides with the central portion of the down warp zone and which is more of a syncline orium feature. The third zone is the thrusting zone which occupies the northern portion of the Delta and is characterized by the presence of a thrust fault oriented in the northeast direction. According to Shata and El Fayoumy (1969) the sedimentary section in Delta area and its fringes has a thickness of more than 10,000 m of which about 5000 m belong to Neogene.

The Quaternary Nile sediments lie over Pliocene or older sediments (Said, 1990). It constitutes the main water-bearing formations in the Nile delta. These sediments classified into Bilqas formation in the upper and Mit Ghamr formation in the lower. The Bilqas formation belongs to Holocene age and consists mainly of clay and silt. In the south delta, Bilqas formation is relatively thin and coarse; its thickness ranges between 15 and 25 m. Toward the north it becomes thick and fine, its thickness reaches more than 50 m. Bilqas formation shows distinct lateral variation from sand or silt facies in the south to clay facies in the north (El-Fayoumi, 1987) as shown in study area of Fig. 1. Mit Ghamr Formation of Pliocene–Pleistocene constitutes the main aquifer of the Nile delta. It consists mainly of sand and gravel with occasionally thin clay interactions. The sand and gravel are more common in the southern part where clay is dominant in the north with occasional discontinuity and interaction of sand and gravel. The thickness of Mit Ghamr formation gradually increases toward the north and northeast. It ranges from 100 to 400 m in the south, from 500 to 700 m in the middle and reaches maximum thickness exceeding

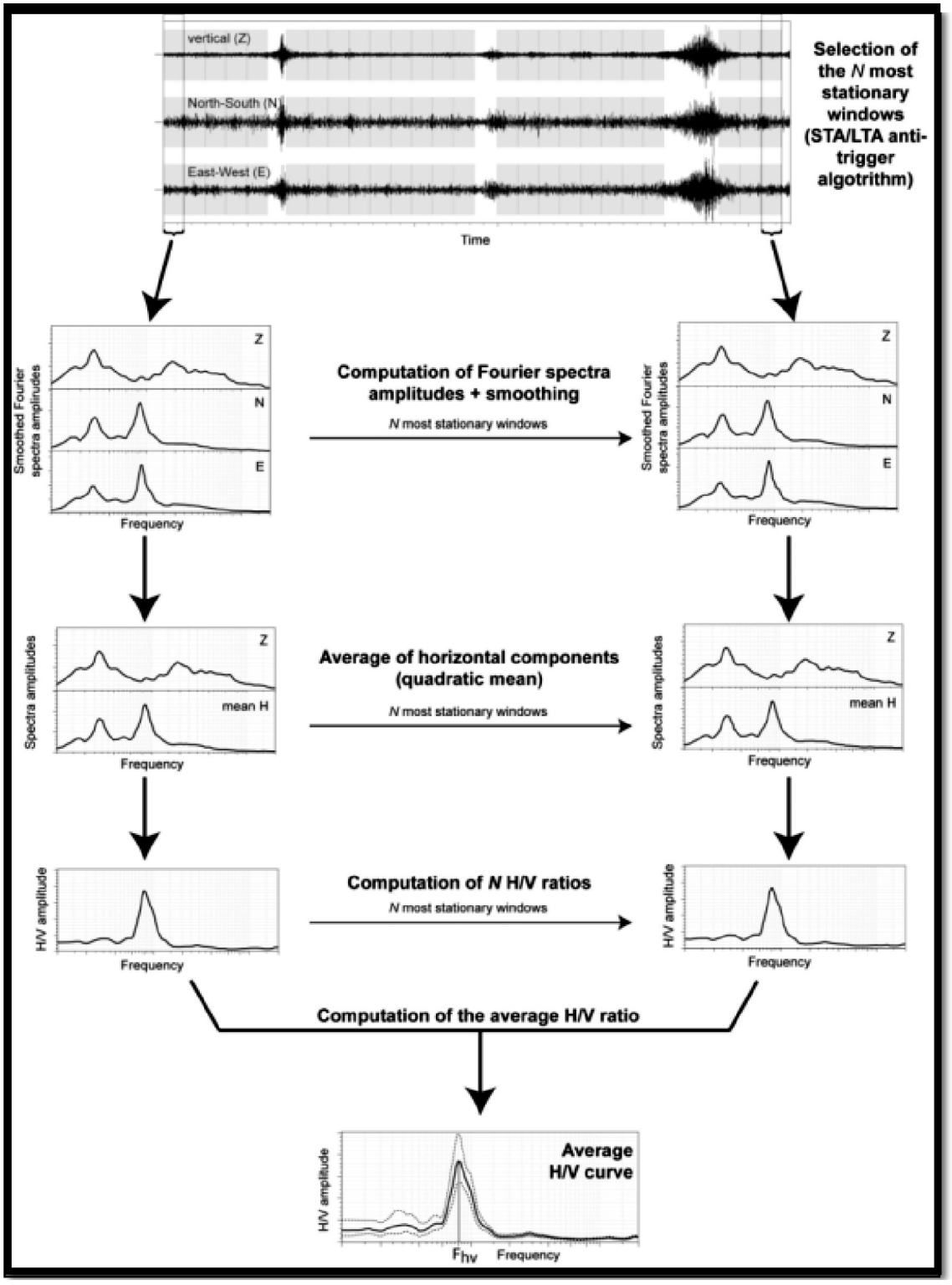

Fig. 3. Flowchart shows the computation steps of the H/V ratio (http://www.geopsy.org/documentation/geopsy/hv.html).

900 m in the north (Serag El-Din, 1989). Fig. 2 shows a longitudinal cross section of the Nile delta was developed by Elewa (2010).

3. Data analysis and processing

This study used the microtremor measurements of 120 sites in Nile delta that conducted by the authors and professional work team of National Research Institute of Astronomy & Geophysics in 2006. Fergany and Bonnefoy-Claudet (2009) discussed the data acquisition in detail. The measurements were done using two broadband seismological stations individually on three parallel profiles as shown in Fig. 1. Although these measurements were processed and analyzed using JSsesame tool (http://jsesame.software.informer.com) by Fergany and Bonnefoy-Claudet (2009), we reprocessed it again using GEOPSY code, progressively, more conventional techniques are included to offer a high quality data

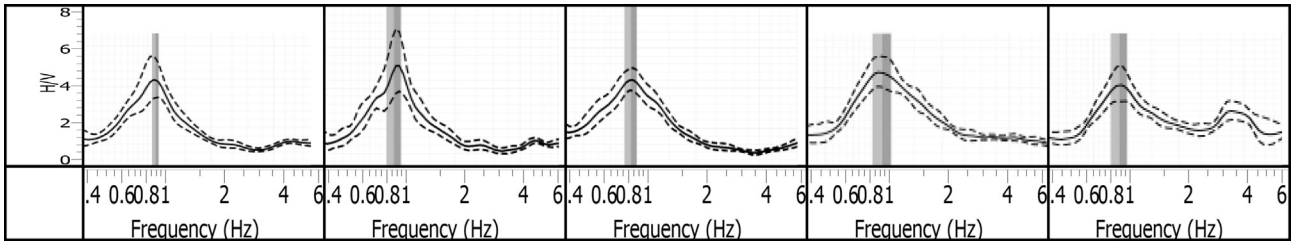

Fig. 4. An example of the microtremor H/V curves. Dashed lines are the maximum and minimum amplification and continuous line is the average amplification value.

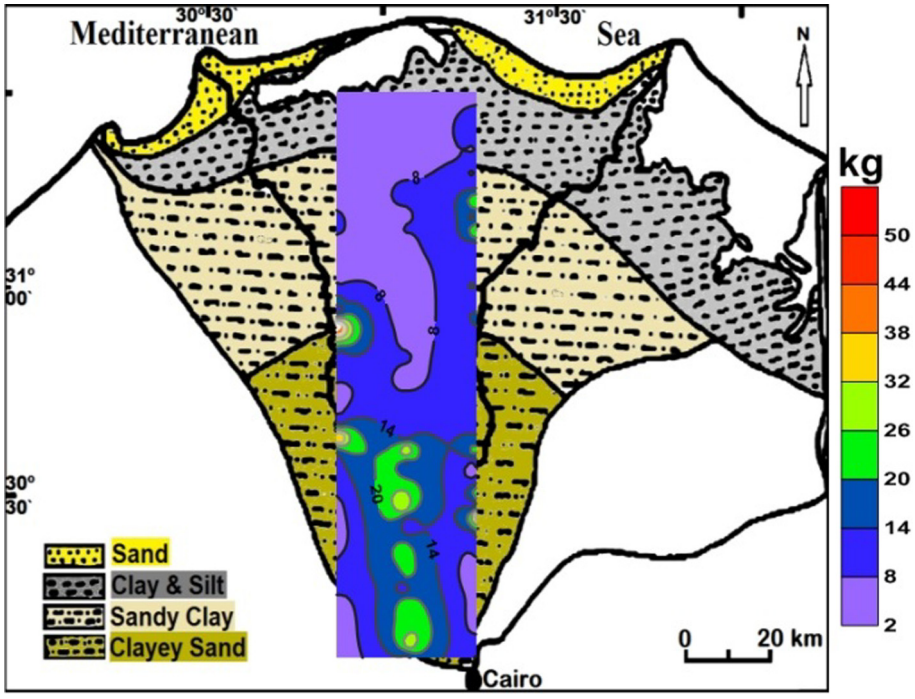

Fig. 5. Contour map of the fundamental frequency peak derived from HVSR.

Table 1
Strain dependence of dynamic properties of soil (Ishihara, 1978).

Size of Strain γ	10^{-6} 10^{-5}	10^{-4}	10^{-3}	10^{-2} 10^{-1}
Phenomena	Wave, Vibration	Crack, Settlement		Land slide, Soil Compaction, Liquefaction
Dynamic Properties	Elasticity	Elasto-Plasticity		Collapse
				Repeat- Effect, Speed- Effect of Loading

processing (http://www.geopsy.org). The main purpose of reprocessing data is using advanced tool to enhance the natural signal and minimize the artificial noise that may be included in the previous results of Fergany and Bonnefoy-Claudet (2009). The computation of the H/V ratio was described in Fig. 3 that follows different steps: (a) record a 3-component ambient noise signal, (b) select of the most stationary time windows, (c) compute and smoothing of the Fourier amplitude spectra for each time windows, (d) average the two horizontal component, (e) compute the H/V ratio for each window and (f) compute the average H/V ratio.

The clarity and stability of the H/V peak frequency value and curve are the first requirements concern the reliability of the H/V results. Reliability implies stability, i.e., the fact that actual H/V curve obtained with the selected recordings, be representative of H/V curves that could be obtained with other ambient vibration recordings and/or with other physically reasonable window selection. Processing of 120 free-field microtremor measurements in

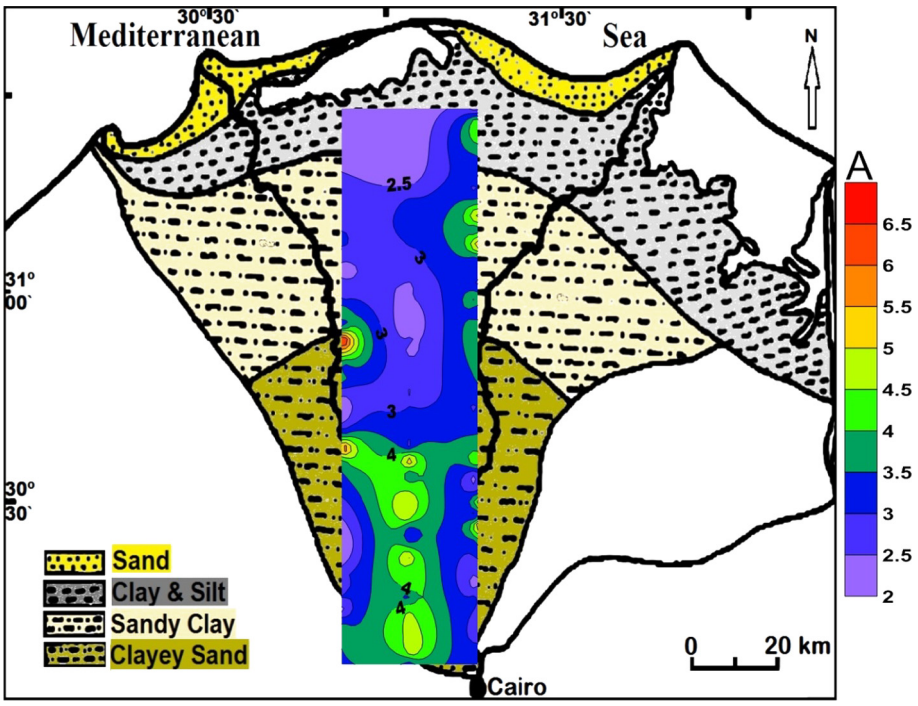

Fig. 6. Contour map of the peak amplitudes derived from HVSR.

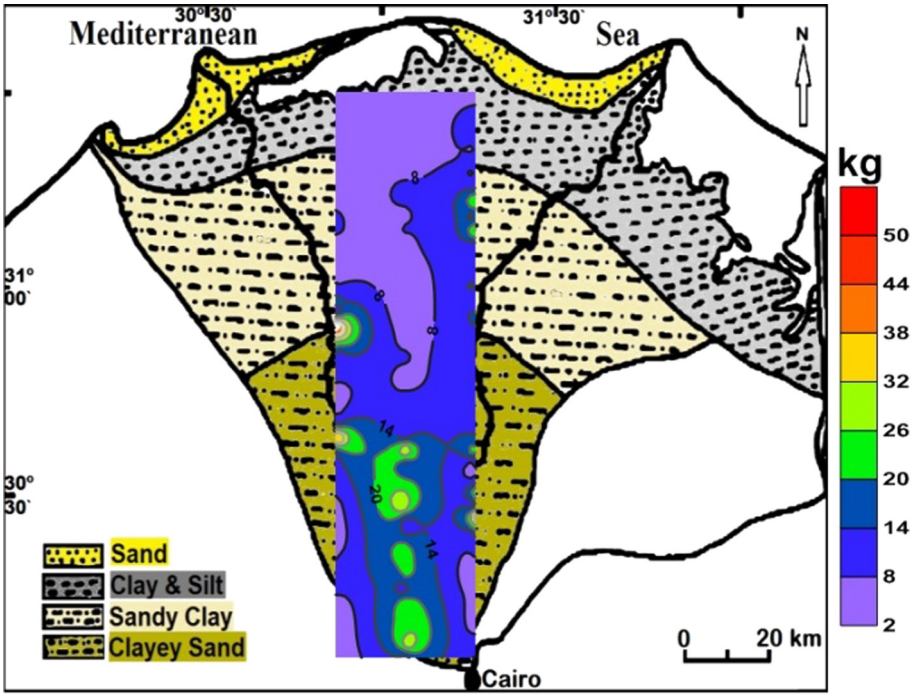

Fig. 7. Contour map of the K_g index derived from HVSR results (Fig. 4 and 5).

the Nile delta showed that 96 of them fulfilled the nine criteria defined and discussed in detail by SESAME (2004) for reliable results of H/V peak frequency and curve. The main reason for disregarding the other 24 measurements is the parameter that may influence H/V results without possible control, such as nearby structures, underground structures, or in situ soil-sensor coupling.

Fig. 4 shows an example of the reprocessed HVSR amplification with picking the fundamental frequency at Nile delta. The frequencies of peaks determined at 96 points were graphed in Fig. 5 as a contour map of the fundamental frequency. The frequencies of the observed HVSR peaks are distributed in the range of 0.75–4.6 Hz, but most of them (61 points) are in the range 0.75–1 Hz, and 33 points are below 2 Hz and only two points above 2 Hz. The amplitude of the HVSR peaks were picked at the 96 points and used for contouring a map of the amplification of sediments in the Nile delta (Fig. 6). These amplifications are distributed in the wide range of 2–7, but most of them (57 points) are in the range 3–5. If we correlate the fundamental frequency and amplification maps (Figs. 5 and 6), we noted that the high amplitudes joined to the low frequencies, as it is a remarkable in the south Nile delta.

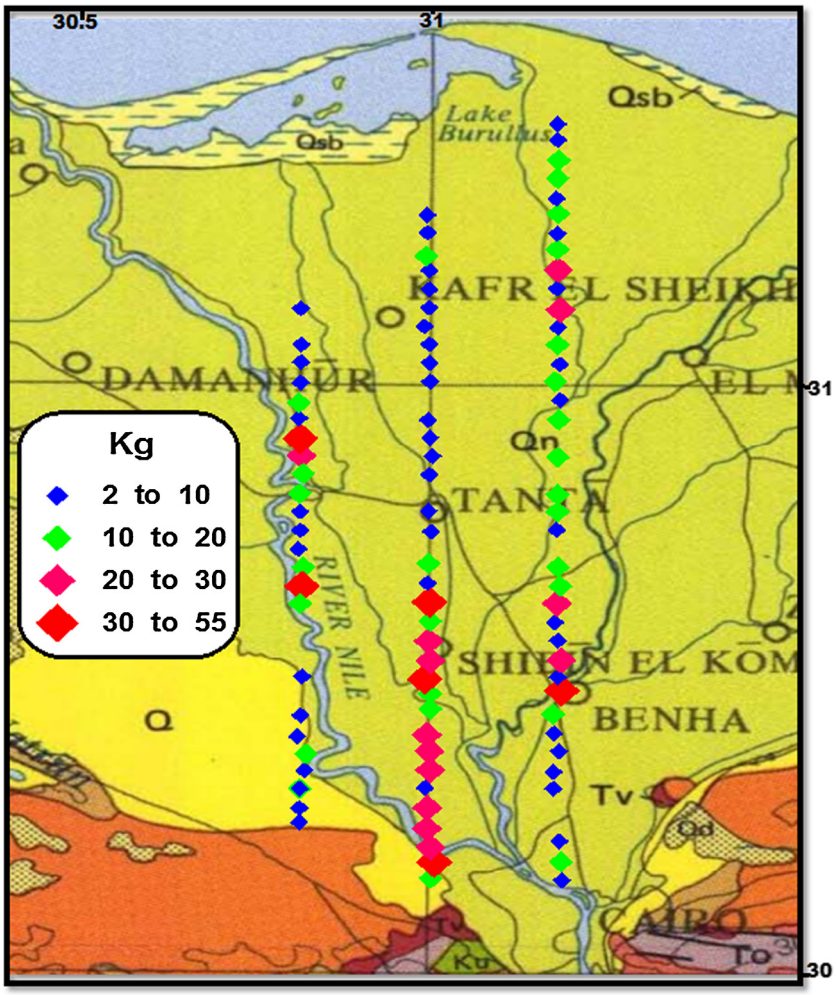

Fig. 8. Classed map of K_g index in the Nile delta basin.

The results of this study, Figs. 5 and 6 were compared with that obtained by Fergany and Bonnefoy-Claudet (2009), Fig. 6. We can appreciate that more a distinctive variation in F_0 and A_0 from south and north of delta basin in this study.

4. Assessment of liquefaction potential

HVSR has been widely used to estimate the natural frequency and soil amplification (Nakamura, 1997, 2000, 2008; Bard, 1999; Gosar, 2007; Fergany and Bonnefoy-Claudet, 2009). The main advantages of HVSR method are easy to use in anytime and anywhere, low-cost measurement, and estimate the frequency of sediment directly without having to know the geology and shear wave velocity structure beneath the surface using inversion tool (Herak, 2008; Triwulan et al., 2010; El-Hady et al., 2011). Further, the use of microtremor was later expanded to identify the vulnerability index for ground (Nakamura, 1996, 1997, 2000, 2009; Daryono et al., 2009).

Vulnerability index for ground (K_g) is derived from strains of ground (γ) in time of earthquakes (Nakamura, 1997) as follow:

$$\gamma = K_g \times \alpha b \ [\text{in } 10^{-6}] \ \& \ K_g \cong A_g^2/F_g \ [\text{in } 10^{-6}] \quad (1)$$

where αb is the acceleration of basement ground, A_g is amplification factor, F_g is the proper predominant frequency of surface ground.

Based on the above equation, the effective strain can be estimated by multiplying K_g value with maximum acceleration of basement ground α_b in Gal (=cm/s^2) and can be considered as an index to indicate easiness of deformation of measured points, which is expected to be useful to detect weak points of the ground.

Table 1 shows relationship of shear strain γ to ground disasters compiled by Ishihara (1978). It indicates that from $\gamma = 1000 \times 10^{-6}$ ground begins to show non-linear character and in $\gamma > 10{,}000 \times 10^{-6}$ large deformation and collapse occur.

The authors applied this method to the microtremor observation sites in Fig. 1 and HVSR results were presented in Figs. 5 and 6 for calculating K_g values. The K_g values have a wide range from 3 to 53. Fig. 7 shows a contour map of K_g values. We appreciated that the K_g values are over than 20 in the southern part of the basin and the highest K_g values joint to the places adjacent to the branches of the river. However, the smallest K_g values (<12) are common in the central of the basin toward the north direction.

5. Results and discussion

A reprocessing of microtremor measurements that were carried out in 2006 was done using Geopsy code for calculating HVSR of each observation point in the Nile Delta basin. Amplification factors and fundamental frequencies were estimated and presented in contour maps (Figs. 5 and 6), where A varies from 2 to 7 and F ranged from 0.75 to 4.6 Hz. The large amplification and low frequencies are common in the southern part of the Nile Delta. The amplification factor and fundamental frequency were used to calculate the K_g value for assessing the potential liquefaction in the basin. The K_g values were presented in a contour map

(Fig. 7), where its value varies widely from place to place entire the basin. The higher values of K_g (>20) are generally common in the southern part of the Nile delta in relative to that in the northern part. To estimate the worst potential liquefaction places, we presented K_g values in a classed map (Fig. 8). The worst potential liquefaction zones ($K_g > 30$) are frequently joined to the Damietta and Rosetta Nile River branches and south Delta.

To interpret these significant results, we discussed the HVSR and K_g values in view of the stratigraphic lithology and geologic setting of the Nile Delta. Nile Delta is the unique site in Egypt that is favored for accumulation and preservation of the Quaternary sediments (Said, 1981). The Quaternary subsurface section of the Nile Delta has been subdivided by many authors (Said, 1981; De Wit and Van Stralen, 1987; Zaghloul et al., 1977) into two rock units on the basis of their lithological composition. The section includes from base to top Mit Ghamr and Bilqas formations (Rizzini et al., 1978). The Mit Ghamr formation (are mainly sands with clay and gravel interbeds with middle Pleistocene age (Said, 1981). The thickness of Mit Ghamr formation gradually increases toward the north and northeast. It ranges from 100 to 400 m in the south, from 500 to 700 m in the middle and reaches maximum thickness exceeding 900 m in the north (Serag El-Din, 1989). Bilqas formation (Holocene) is dominated by sand, silt and clay interbeds; the sediments are more calcareous in the northern part of the Nile Delta. Also peat layers have been encountered within the sediments of the Bilqas formation. The maximum thickness of this formation is about 77 m (Zaghloul et al., 1977). According to the latitudinal and longitudinal cross sections of Fig. 2, the geological units of the Nile Delta aquifer are as follows: (a) Top unit of Holocene clay aquitard, (b) Quaternary (Pleistocene) and late Tertiary gravel and sand unit (aquifer) and (c) Basal unit of Pliocene clay aquiclude.

We compared the fundamental frequency and amplification contour maps in Figs. 5 and 6 with the general sediments thickness. Unexpected results of increasing fundamental frequency and decreasing amplification are common toward the north of the Nile delta; however, the thickness of sediments increases from 200 m in the south to ~1000 m in the north. To understand these surprising results, we compared F and A contour maps with sediment units of the longitudinal cross section in Fig. 2. We inferred that the relatively lower F ($\leq$1 Hz) values, in the south delta, are due to response to the whole Holocene and Pleistocene formations (~200 m), where the texture of the lithostrategraphic units is similarly, and the higher A values are due to the high impedance ratio between Pleistocene and Pliocene formations. However, the higher F values to the north delta are due the response to the Holocene formation only (~50 m) and the lower A values are due to the low impedance ratio between Holocene and Pleistocene formations. Based on F and A values in Figs. 5 and 6, lithostratigraphic map (Fig. 1), and longitudinal cross section of the Nile Delta (Fig. 2), K_g index values (Figs. 7 and 8) are in a good agreement with fluvial plain of Nile delta. Where, it is commonly known that liquefaction susceptibility of sand is more than that of clay; clay is more resistance for liquefaction during cyclic earthquake. We concluded that the worst potential liquefaction zones ($K_g > 30$) are frequently joined to the Damietta and Rosetta Nile River branches and south Delta. Based on Eq. (1) and Table 1, we concluded that any earthquake shakes the ground with acceleration more than 50 gal at hard rock can cause a perceived deformation of sandy sediments, and liquefaction can take place in the weak zones of $K_g \geq 20$. The HVSR is a sensitive technique for lithological stratigraphy variations in two dimensions and can be used as a powerful tool for microzonation studies.

Acknowledgments

The authors acknowledge that the National Research Institute of Astronomy & Geophysics full supported the data used in this work. Authors would like to thank all staff of Seismology department, National Research Institute of Astronomy & Geophysics, for data measurements. The authors highly benefited from helpful discussions Yutaka Nakamura and Lawrence Hutchings.

References

Bard, P.Y., 1999. Microtremor measurements: a tool for site effect estimation? In: Irikura, K., Kudo, K., Okada, H., Sasatami, T. (Eds.), The Effects of Surface Geology on Seismic Motion. Balkema, pp. 1251–1279.

Daryono, Sutikno, Sartohadi, J., Dulbahri, Brotopuspito, K.S., 2009. Efek Tapak Lokal (local site effect) di Graben Bantul Berdasarkan Pengukuran ikrotremor. In: International Conference Earth Science and Technology, Yogyakarta 6–7 August 2009.

De Wit, H.E., Van Stralen, L., 1987. Preliminary results of the paleogeographical survey. In: Van Den Brink, E.C.M. (Ed.), The Archaeology of the Nile Delta, Wolfkamb, Amsterdam, pp. 135–139.

Duval, A.-M., Chatelain, J.-L., Guillier, B. SESAME WP02 team, 2004. Influence of experimental conditions on H/V determination using ambient vibrations (noise). In: 13th World Conf. on Earthq. Engin. Paper No. 306.

El-Sayed, A., Arvidsson, R., Kulhánek, O., 1998. The 1992 Cairo earthquake: a case study of a small destructive event. J. Seismol. 2 (4), 293–302.

El-Sayed, A., Vaccari, F., Panza, G.F., 2001. Deterministic seismic hazard in Egypt. Geophys. J. Int. 144, 555–567.

Elewa, H.H., 2010. Potentialities of water resources pollution of the Nile river delta, Egypt. Open Hydrol. J. 4, 1–13.

El-Fayoumi, I.F., 1987. Geology of the Quaternary Succession and Its Impact on the Groundwater Reservoir in the Nile Delta Region. Bull Faculty of Science, Mansoura University, Egypt.

El-Hady, S., Fergany, E., Othman, A., ElKareem, G., 2011. Seismic microzonation of Marsa Alam, Egypt using inversion HVSR of microtremor observations. J. Seismol. 9 (1). http://dx.doi.org/10.1007/s10950-011-9249-4.

Herak, M., 2008. Model HVSR—a Matlab tool to model horizontal-to-vertical spectral ratio of ambient noise. Comput. Geosci. 34, 1514–1526.

Fergany, E., Bonnefoy-Claudet, S., 2009. Microtremor measurements in the Nile delta basin, Egypt: response of the topmost sedimentary layer. Seismol. Res. Lett. 80 (4), 591–598.

Galloway, W.E., 1975. Process framework for describing the morphologic and stratigraphic evolution of deltaic depositional systems. In: Broussard, M.L. (Ed.), Detas, Models for Exploration. Houston Geological Society Houston, TX, pp. 87–98.

Geopsy Software, 2012. Geopsy.org packages, release 2.5.0, win32. <http://www.geopsy.org/download.php>.

Gosar, A., 2007. Microtremor HVSR study for assessing site effects in the Bovec basin (NW Slovenia) related to 1998 Mw5.6 and 2004 Mw5.2 earthquakes. Eng. Geol. 91, 178–193.

Ishihara, K., 1978. Introduction to Dynamic Soil Mechanism.

Nakamura, Y., 1989. A method for dynamic characteristics estimation of subsurface using microtremor on the ground surface. Q. Rep. Railway Tech. Res. Inst. 30 (1), 25–33.

Nakamura, Y., 1996. Real time information systems for seismic hazards mitigation UrEDAS, HERAS and PIC. Q. Rep. RTRI 37 (3), 112–127.

Nakamura, Y., 1997. Seismic vulnerability indices for ground and structures using microtremor. In: World Congress on Railway Research in Florence, Italy, November 1997.

Nakamura, Y., 2000. Clear identification of fundamental idea of Nakamura's technique and its applications. 12WCEE, 2656, Auckland, New Zealand.

Nakamura, Y., 2008. On the H/V spectrum. In: The 13th Word Conference on the Earthquake Engineering, Beijing, China, October 12–17.

Nakamura, Y., 2009. Basic structure of QTS (HVSR) and examples of application. In: Increasing Safety by Combining Engineering Technologies and Seismological Data. NATO Science for Peace and Security Series C: Environmental Security. Springer.

Rizzini, A., Vezzani, F., Cococetta, V., Milad, G., 1978. Stratigraphy and Sedimentation of Neogene – Quaternary Section in the Nile Delta Area Exploration Seminar. I.E.C., Cairo.

Said, R., 1981. The Geological Evolution of the River Nile. Springer, New York, N.Y. 151 pp.

Said, R., 1990. The Geology of Egypt – 734 pp. A. Balkema Publishers, USA.

Shata, A.A., El Fayoumy, I., 1969. Remarks on the regional geological structure of the Nile delta. In: Proc. of Bucharest Symposium for Hydrology of the Delta.

Serag El-Din, H., 1989. Geological and Hydrogeological and Hydrological Studies on the Quaternary Aquifer Ph.D. dissertation. Fac. of Sci., Mansoura Univ., Mansoura, Egypt.

Triwulan, W., Utama, D., Warnana, D., Sungkono, 2010. Vulnerability index estimation for building and ground using microtremor. In: Proceedings of International Seminar on Applied Technology, Science, and Arts (2nd APTECS), Surabaya, 21–22 Dec. 2010, 2086-1931, pp. 1194–1197.

Wright, L.D., Coleman, J.M., 1973. Variations in morephology of major river deltas as functions of ocean wave and river discharges regimes. AAPG Bull. 57, 370–398.

Zaghloul, Z.M., Essawy, M.A., El-Sherbini, 1977. Grainsize and texture analysis of the subsurface sediments of Sidi Salim Well No. 1, Nile Delta, Egypt. Bull. Fac. Sci. 4, 79–98.